TECHNICAL MEMORANDUM

624

Sensitivity of L-Band NWP forward modelling to soil roughness

J. Muñoz Sabater, P. de Rosnay and G. Balsamo

Research Department

In review for International Journal of Remote Sensing

April 2010

European Centre for Medium-Range Weather Forecasts
Europäisches Zentrum für mittelfristige Wettervorhersage
Centre européen pour les prévisions météorologiques à moyen terme

Series: ECMWF Technical Memoranda

A full list of ECMWF Publications can be found on our web site under:
http://www.ecmwf.int/publications/

Contact: library@ecmwf.int

Abstract

This paper investigates the sensitivity of the European Centre for Medium-Range Weather Forecasts (ECMWF) simulated L-band brightness temperatures (TB) in response to different soil roughness parameterisations. To this end, the ECMWF operational conditions during the year 2004 have been used to force the Hydrology Tiled ECMWF Scheme for Surface Exchanges over Land (HTESSEL) coupled to the Community Microwave Emission Model (CMEM). The coupled HTESSEL-CMEM system is then run at five different incident angles ($20^\circ, 30^\circ, 40^\circ, 50^\circ$ and 60°) and for five soil roughness parameterisations available in CMEM. The performance of the simulated TB are analysed at ground point scale over the Surface Monitoring Of Soil Reservoir EXperiment (SMOSREX) site in South West of France. For this particular data set, both ground-based vertical profile of soil moisture and L-band radiometric observations are available for evaluation of the ECMWF forecast system nearest grid box. In particular, the results show that the simple Choudhury parameterisation best fits the observations for both horizontal (H-pol) and vertical polarisation (V-pol) and for most of the incidence angles tested. The best forward modelling configuration is at 50° for the V-pol, with coefficient of determination between modelled and observed TB of 82.9% and root mean squared error of 7.9 K. The sensitivity of the L-band TB errors to the empirical soil roughness parameter is also investigated. Strong sensitivity to this parameter is shown, mainly at H-pol for the least rough surfaces. The investigation carried out in this paper gives an insight into the soil roughness model to be used in the operational configuration of the CMEM L-band forward operator, for the future assimilation of the Soil Moisture and Ocean Salinity satellite data of the European Space Agency.

1 Introduction

The Soil Moisture and Ocean Salinity (SMOS) mission of the European Space Agency (ESA) Kerr et al. (2001) is a response to a) the lack of a ground-based global homogeneous network of soil moisture measurements and b) the growing need for an accurate estimation of the root-zone soil water content for short- and medium-range meteorological modelling, hydrological modelling and extreme events forecast such as floods. SMOS is expected to be fully operational during the year 2010, providing for the first time global coverage of the earth natural microwave emission in L-band, where the signal is the most sensitive to the superficial soil water content. As a Numerical Weather Prediction (NWP) centre, the European Centre for Medium-Range Weather Forecasts (ECMWF) is implementing the direct assimilation of near real time brightness temperatures (TB) in L-band over snow-free areas. The generation and a posteriori assimilation of a soil moisture retrieval product would cause a latency incompatible with NWP time constraints. The assimilation of SMOS TB observations is expected to enhance significantly the forecast skill, both at short Drusch and Viterbo (2007) and medium range Fischer et al. (2007), by providing accurate soil moisture initial conditions for NWP systems.

The assimilation of observed TB data will only be effective if realistic and dynamically consistent fields of TB are simulated as a function of the land surface conditions. In this context ECMWF has developed the Community Microwave Emission Model (CMEM) forward operator for low frequency passive microwave TB (from 1GHz to 20 GHz) of the surface Drusch et al. (2009); Holmes et al. (2008). The CMEM forward operator is designed to have a highly modular structure, accounting for the soil, vegetation, snow and atmosphere natural emissions contributing to the top of the atmosphere TB. For each component of the emission model, a choice of different parameterisations is available, which guarantees great flexibility with regard to the combination of all the model choices. Furthermore, it is straightforward to integrate state of the art parameterisations for each component of the emission model. Based on spaceborne observations from the S-194 passive microwave radiometer onboard the Skylab space station, Drusch et al. (2009) showed that the Kirdyashev et al. (1979) model was best adapted to simulate the vegetation opacity effect on the L-band radiometric signal in several regions of North and South-America. This result was confirmed by de Rosnay et al. (2009) for the African Monsoon Multidisciplinary Analysis (AMMA) Land Surface Intercomparison Project (ALMIP), who performed an intercomparison exercise of several land surface models at regional scale for a complete annual cycle. Concerning soil roughness, although the study of Drusch et al. (2009) provided a first indication of the possible (calibrated) value of soil roughness parameter at continental scale, the number of roughness models used was very limited, whereas the de Rosnay et al. (2009) study was undertaken at C-band and thus just one roughness model implemented in CMEM was applicable. However, soil roughness remains one of the most important parameters to affect forward TB in L-band. Choudhury et al. (1979) indicated that the roughness effect on brightness temperature for wet soils could be as large as 50 K when compared with a smooth surface. In general, surface roughness decreases the soil reflectivity (thus increasing the brightness temperature) and the difference between the vertical and horizontal polarization. Furthermore as the surface roughness increases, the sensitivity of brightness temperatures to soil moisture is reduced Engman and Chauhan (1995); Njoku and Entekhabi (1996). Soil roughness is however difficult to measure and only a few field experiments provide local estimates of roughness values for validation. For global scale applications it still remains unknown, whereas it will be a crucial parameter to account for NWP applications.

Therefore, based on the significant influence of soil roughness in the forward TB, this paper focuses on this component, and investigates the response of ECMWF simulated L-band TB errors (background error) to different soil roughness microwave modelling approaches implemented in CMEM. The year 2004 was selected due to its very contrasted climatic conditions, with an average wet winter, a very dry summer and autumn and an unusual double cycle of vegetation. Furthermore, by using just a year of data the atmospheric forcing used in this study is obtained under the same ECMWF operational conditions. Several one-year simulations are generated at $\sim 25km$ horizontal spatial resolution (T799 spectral resolution) using different choices for soil roughness, while keeping the other contributions to the total microwave land surface emission constant in CMEM. Simulated first-guess TB at L-band are validated using the Surface Monitoring Of Soil Reservoir EXperiment (SMOSREX) data set de Rosnay et al. (2006).

2 Methodology

The ECMWF modelled TB in L-band is obtained in two steps: 1) the integration of the ECMWF operational HTESSEL (Hydrology Tiled ECMWF Scheme for Surface Exchanges over Land) land surface scheme Balsamo et al. (2009) during the year 2004 provides the input for the uppermost surface soil moisture and temperature fields for the land emission model and, 2) the CMEM provides multi angular and polarised fields of low-frequency microwave TB fields. Due to the multiple choice structure of CMEM microwave emission components, an important step towards the generation of TB at both polarisation states is the choice of a CMEM configuration. Discussion of these steps as well as the validation approach undertaken in this paper is the objective of this section.

2.1 CMEM configuration and soil roughness model

CMEM physics is based on the parameterisations used in the L-Band Microwave Emission of the Biosphere Wigneron et al. (2007) and Land Surface Microwave Emission Model Drusch et al. (2001). Several parameterisations for soil dielectric constant, effective temperature, soil roughness, vegetation opacity and atmospheric contribution are considered. In this study the vegetation opacity model of Kirdyashev et al. (1979) is used, in combination with the Wang and Schmugge (1980) dielectric model and the Wigneron et al. (2001) effective temperature model. The atmospheric contribution is accounted for as in Pellarin et al. (2003). This combination of parameterisations has been shown to be well suited for TB modelling Drusch et al. (2009); de Rosnay et al.

(2009).
For soil roughness, physically-based models have recently been proposed Shi et al. (2002); Schneeberger et al. (2004), some of which have addressed roughness in L-band at different scales. However their usage at global scale is complicated by the high number of parameters involved, the significant computing burden and the need for detailed ground truth information. In this context, semi-empirical approaches are best adapted to be implemented for NWP applications.
In CMEM five parameterisations are available to model the effect of soil roughness with a minimum number of parameters. A semi-empirical approach was proposed by Wang and Choudhury (1981) to represent soil roughness effects on the microwave emission as a function of the smooth emissivity $r_{s,p}$ and three parameters Q, h, and N:

$$r_{r,p} = (Q \cdot r_{s,p} + (1-Q) \cdot r_{s,q}) exp(-h \cdot cos^N \Theta)$$

where q and p refer to the polarisation states, Q is the polarisation mixing factor, N describes the angular dependence, h is the roughness parameter and Θ is the incidence angle. The mixing factor Q is considered to be very low at low frequencies and generally set to 0 at L-band. Most of the models considered in this study Wigneron et al. (2001); Choudhury et al. (1979); Laboratories (2007); Wigneron et al. (2007) at L-band are based on the previous equation (the so called "*Q-h,N*" parameterisation) and they differ from the different approaches used to model the N and h parameters. While the Choudhury et al. (1979) approach is the simplest model as the soil roughness parameter h is controlled by only two parameters, Wigneron et al. (2001); Laboratories (2007) and Wigneron et al. (2007) are more complex and they include dependencies on other physical parameters and soil properties, as the correlation length, the clay fraction or the superficial soil moisture (see Table 1). Only Wegmüller and Mätzler (1999) have chosen a different approach in which the V-pol depends on the computed H-pol expressed only as a function of h and Θ:

$$\begin{aligned} r_{r,H} &= r_{s,H} \cdot exp\left(-h^{\sqrt{0.1 \cdot \cos\Theta}}\right) \\ r_{r,V} &= r_{r,H} \cdot \cos^N \Theta \qquad (\text{only for } \Theta < 60^\circ) \end{aligned}$$

Table 1 presents the value of the parameter N and the h approach, for each of the soil roughness models tested at L-band and for the fallow type vegetation considered in this study.

*Table 1: Soil roughness parameterisations available in CMEM, particularized for L-band and C3-grass vegetation type. In this table '**N**' is the parameter expressing the angular dependence of soil emission to soil roughness, '**h**' is the soil roughness parameter, 'H' is H-pol, 'V' is V-pol, σ is the soil roughness standard deviation of height, L_c is the correlation length, k is the wave number, 'w_p' is the wilting point, 'wf_c' is the field capacity, 'f_{CLAY}' is the soil clay fraction and 'w_g' is the superficial soil moisture*

Soil roughness model	**N**	**h**
(Wigneron et al., 2001)	$N_H = 0$ $N_V = 0$	$1.3972 \cdot (\sigma/L_c)^{0.5879}$
(Choudhury et al., 1979)	$N_H = 0$ $N_V = 0$	$(2k\sigma)^2$
(Wegmüller and Mätzler, 1999)	0.655	$k\sigma$
(Laboratories, 2007)	$N_H = 1$ $N_V = 0$	$w_t = 0.49 \cdot w_p + 0.165$ $w_{fc} = w_t + 0.10 \cdot f_{CLAY}$ if $w_t < w_g < w_{fc}$, $h = 0.1 - (0.05 \cdot \frac{w_g - w_t}{w_{fc} - w_t})$ if $w_g < w_t$, $h = 0.10$
(Wigneron et al., 2007)	$N_H = 1$ $N_V = 0$	$1.3 - 1.13 \cdot w_g$

2.2 ECMWF background L-band TB

The set-up of the experiments carried out in this paper reproduces the ECMWF operational configuration in the year 2004 at $\sim$ 25 km horizontal spatial resolution. The land surface scheme HTESSEL is forced at 30 min time step with meteorological fields of surface pressure, specific humidity, air temperature and wind speed at the lowest atmospheric level. The instantaneous forcings are linearly interpolated in time from the operational 3 hours resolution short range forecasted fields. The surface radiation and precipitation flux represent 3-h averages, and they are kept constant over a 3-h period to ensure conservation. The integration of HTESSEL in 2004 provides the uppermost surface soil moisture and soil temperature fields (within the first soil 7 cm), as well as snow depth and snow density fields, which are then coupled with CMEM to simulate ECMWF first-guess L-band TB. Additional land surface information needed is soil texture data obtained from the Food and Agriculture Organization (FAO) data set, whereas sand and clay fractions have been computed from a lookup table according to Salgado (1999). The soil roughness standard deviation of height (σ) parameter in CMEM is set to 2.2 cm as in Holmes et al. (2008). Vegetation type and leaf area index (LAI) are derived from the ECOCLIMAP database Masson et al. (2003), which is also used to derive the vegetation water content for grasslands and crops. The coupled HTESSEL-CMEM system is then run at five different incident angles ($20^\circ, 30^\circ, 40^\circ, 50^\circ$ and 60°) and for five soil roughness parameterisations available in CMEM. Thus, 25 computed 1D time series of the ECMWF first-guess L-band TB for the year 2004 are obtained for both horizontal and vertical polarisation.

2.3 Validation approach

In order to evaluate the performance of the ECMWF forecast system of background L-band TB, a set of independent observations is needed. Apart from a few historic observations over North and South-America at 110 km resolution from the S-194 passive microwave radiometer onboard the Skylab space station in 1973 Eagleman and Lin (1976), only a few field experiments provide accurate L-band radiometric measurements. In this study the simulated ECMWF first-guess TB at L-band are evaluated against in-situ radiometric observations of the Surface Monitoring Of Soil Reservoir EXperiment (SMOSREX) data set de Rosnay et al. (2006). SMOSREX was selected since it currently contains one of the most consistent and continuous data sets of radiometric L-band observations over natural grass at different incident angles. This field experiment was designed with the main objectives of modelling the microwave emission at L-band de Rosnay et al. (2006); Escorihuela et al. (2007), improving the SMOS retrieval algorithm Laboratories (2007); Saleh et al. (2006) and assimilation of multi-spectral remote sensing data Sabater et al. (2007, 2008). On this site, measurements at L-band have been obtained on a regular basis since January 2003 by the LEWIS (L-band radiometer for Estimating Water In Soils) radiometer Lemaitre et al. (2004) over two samples of fallow and bare soil at both horizontal (H-pol) and vertical polarisaton (V-pol). In this study only the fallow land sample is considered. The L-band radiometer scans the surface at different incidence angles ($20^\circ, 30^\circ, 40^\circ, 50^\circ$ and 60°) but with different temporal sampling. While background TB are obtained with a sampling time of one hour, the time frequency of the observed TB depends on the incidence angle (observations are available every 10 minutes at 40° incidence angle, whereas the fallow sample is sensed twice every 3 hours for the rest of the incidence angles). Both simulated and observed TB data sets are collocated in time (permitting a maximum time difference of 30 minutes) in order to allow a quantitative comparison.

2.4 CMEM main input forcing fields

In this paper, simulated L-band TB from the coupled HTESSEL-CMEM system in a numerical grid box of approximately 25x25 km are compared against point-scale observations. The validation approach is then limited by the different spatial scale of simulated and observed data sets. In order to validate the comparison, the

CMEM main input forcing fields are analysed and compared against in-situ data. Jones et al. (2004) classified the main variables and parameters which input the passive microwave land surface emission models according to their impact on the modelled top of the atmosphere TB. They found that the variables which had the biggest impact in the modelled radiometric signal are related to volumetric soil moisture, vegetation opacity, soil roughness and soil temperature, respectively.
In Fig. 1, the observed superficial volumetric soil moisture (in the first 7cm) in the SMOSREX site is overlapped to the CMEM input soil moisture field for the corresponding ECMWF forecast model grid box. It is shown that the ECMWF forecasted soil moisture captures very well the temporal dynamics of the observations, obtaining thus a very good coefficient of determination ($R^2 = 0.80$) between both data sets for the year 2004. However, the summer and first half of autumn of the year 2004 were exceptionally dry, obtaining in-situ volumetric soil moisture values lower than 0.1 $m^3 \cdot m^{-3}$. HTESSEL is limited by the wilting point value fixed to 0.151 $m^3 \cdot m^{-3}$ (for a medium texture soil as in this study [Balsamo et al. (2009)]), since at lower soil water content evapotranspiration is halted, and thus this dry event is poorly reproduced by the forecasted model at T799 spectral resolution. Even though not shown here, the overestimation of soil moisture in summer consequently penalizes the modelled TB, by decreasing the modelled TB. Fig. 2 shows a scatter plot where soil temperature obtained by HTESSEL (averaged over the first 7 cm) in the SMOSREX pixel is compared to ground-based soil temperature sensors available at 1 and 5 cm. Both data sets show an excellent correlation and a low root mean squared error. Compared to volumetric soil moisture, modelled TB is far less sensitive to initial soil temperature, and errors in this variable have a relatively weak impact in the simulated TB. Concerning the sensitivity to vegetation, for the SMOSREX grid box, up to 93% of the vegetation type is the same as in the SMOSREX vegetation sample. Although not shown here, the low-vegetation type leaf area index used from the ECOCLIMAP database (used as input in CMEM for the vegetation modelling) accurately reproduces the maximum observed in the SMOSREX site. However, the year 2004 showed a double cycle of LAI, obtaining very low or null values of green active vegetation during the dry period. This event is not well reproduced in the ECOCLIMAP data set, which does not take into account interannual variability. An increase in modelled vegetation consequently increases emission due to the vegetated canopy whereas it attenuates the underlying soil emission. This effect is opposite to an overestimation of soil moisture and can partially counteract initial soil moisture errors. Furthermore, Gruhier et al. (2008) showed that superficial soil moisture on the SMOSREX site, located on medium loamy texture soil, slightly overestimated the superficial soil moisture measured by nearby stations presenting different soil texture.

As a result of matching point-scale observations with the model equivalent in a larger numerical grid-box, the previous analysed source of bias should be considered when analyzing the background TB error. In addition, vegetation data does not account for interannual vegetation characteristics. Data assimilation studies in the context of the SMOS mission will have to deal with these limitations. In general, the good correlation shown between the first-guess soil moisture and soil temperature with the ground observations as well as the relatively good representativity of the SMOSREX site within the modelled grid box, make this site suitable to investigate background errors in the simulated ECMWF TB in L-band.

3 L-band TB background error analysis.

3.1 Dependency on soil roughness, incidence angle and polarisation state

It is observed that, for the test period (2004), by using the model proposed by Choudhury et al. (1979) the modelled background TB is the most in agreement with the available validation data set, obtaining the best temporal correlations and the lowest differences for most incidence angles and for both polarisation states (Fig. 3). This

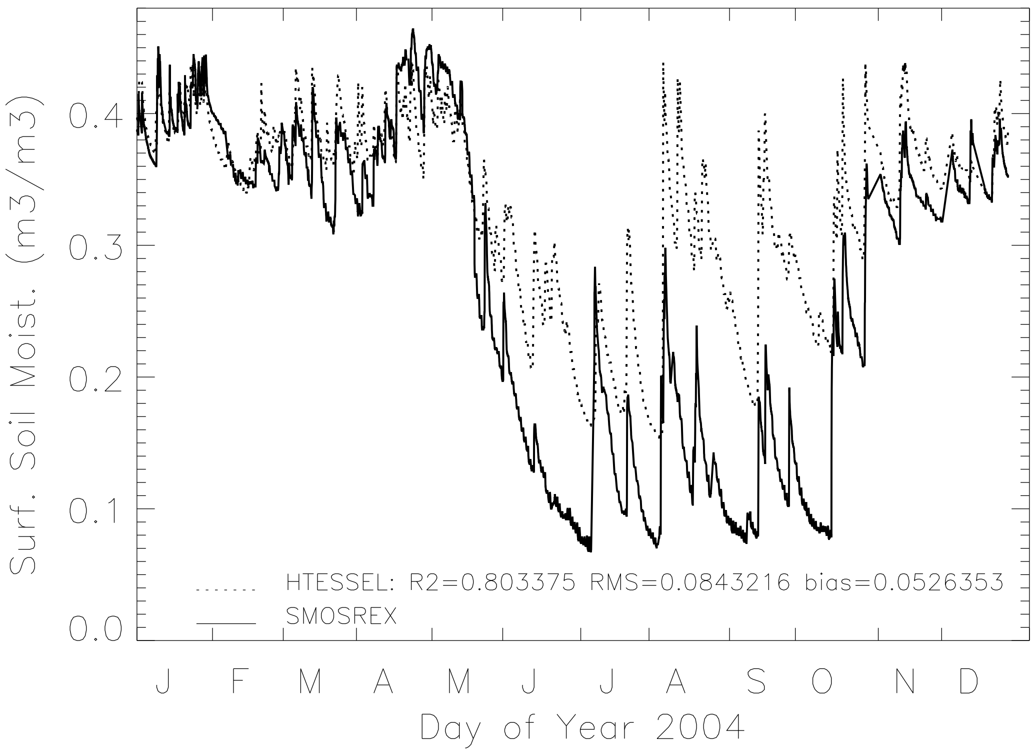

Figure 1: Observed superficial soil moisture at the SMOSREX fallow sample overlapped to simulated superficial soil moisture by HTESSEL land scheme (0-7 cm) at the SMOSREX grid box.

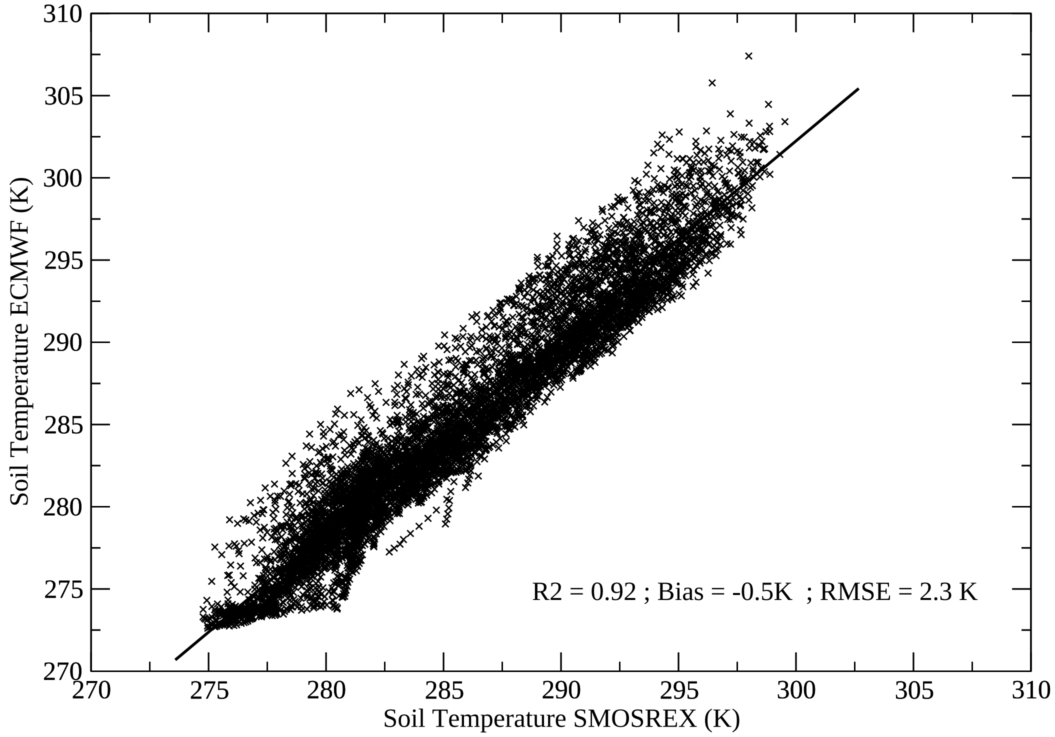

Figure 2: Soil temperature obtained by HTESSEL (0-7cm) forced by ECMWF operational forecast versus SMOSREX ground measurements (mean value based on measurements at 1 cm and at 5 cm), for the year 2004.

figure shows the coefficient of determination (R^2) and the Root Mean Squared Error (RMSE) between the ECMWF modelled background TB in L-band and the observed TB as a function of the incidence angle, at H-pol and V-pol and for five different parameterisations of soil roughness implemented in CMEM (section 2.1). As expected, the background TB in H-pol shows to be very sensitive to the incidence angle, decreasing rapidly the correlation with the observations, as the incidence angle is increased. For this polarisation none of the parameterisations tested produce satisfactory results for large incidence angles, loosing progresively the sensitivity to soil moisture. Radiometric L-band TB in H-pol are very sensitive to soil water content, and at large incidence angles volume effects (as well as roughness and vegetation effects) are more significant and less known, thus these models have not yet found a good fit with the observations. The best configuration at H-pol is Choudhury et al. (1979) at 20° with R^2 72.6% and RMSE 6.6 K. The obtained background TB using the parameterisations depending on soil moisture Wigneron et al. (2007) and soil texture Laboratories (2007) diverge greatly from the observed data set (with RMSE greater than 30 K and thus not shown in the top right panel). This result must be taken with caution since, apart from the significant contribution of the forecast model error to the total background error, at this pixel resolution ($\sim 25 \times 25$ km) the single-point effects might not be well captured or they compensate each other and, at the SMOSREX field site, these effects have been shown to be significant.
The dependency of the TB background errors on the incidence angle is less marked at V-pol for which, in contrast to H-pol, slightly better performances are obtained at all angles, and best at 50°. For angles from 40° to 60° the parameterisations of Choudhury et al. (1979) and Wigneron et al. (2001) have nearly similar performance. In this case the best results are obtained at 50° incidence angle, with R^2 82.9% and RMSE of 7.9 K for the Choudhury et al. (1979) approach and R^2 80.2% and RMSE of 6.7 K for the Wigneron et al. (2001) model.

3.2 Dependency on soil roughness parameter

Several experiments were performed by combining the best modelling and observing configuration using the Choudhury et al. (1979) parameterisation (at 20° incidence angle for H-pol and at 50° for V-pol). The sensitivity of the ECMWF TB background error as a function of the soil roughness standard deviation of height (σ) has been investigated. Fig. 4 shows the RMSE and R^2 between modelled and observed TB for the year 2004 as a function of σ, varying it between 1 and 3 cm. According to table 1 this corresponds, at L-band, to values of the empirical soil roughness parameter between 0.34 and 3.09 for the Choudhury et al. (1979) parameterisation. Background errors in the simulated TB at H-pol show to be very sensitive to soil roughness for σ lower than 2.2 cm. This could be a consequence of the poor knowledge of the effect of soil roughness in the modelled TB at H-pol, mainly for coarse spatial scales where the effect of several soil roughness conditions is present at the same time for a numerical grid box. For soil roughness standard deviation height (σ) 2.2 cm, the TB background error is minimum and equal to 6.6 K. The sensitivity to σ is less marked for the V-pol, however very low values of the roughness parameter (and then a probably underestimation of the soil emissivity) yield larger discrepancy between modelled and observed TB. Nonetheless, as observed in the bottom panel of Fig.2, the best correlations are obtained for σ larger than 2.5 cm (corresponding to a value of h 2.1) and in the same proportion for both polarisation states. In these roughness conditions, forecasted TB are in better agreement with observations in terms of temporal variability and RMSE. Higher values of σ result in small changes in the RMSE and R^2. Therefore the optimal range of the soil roughness parameter is identified to be between 1.67 and 2.15.

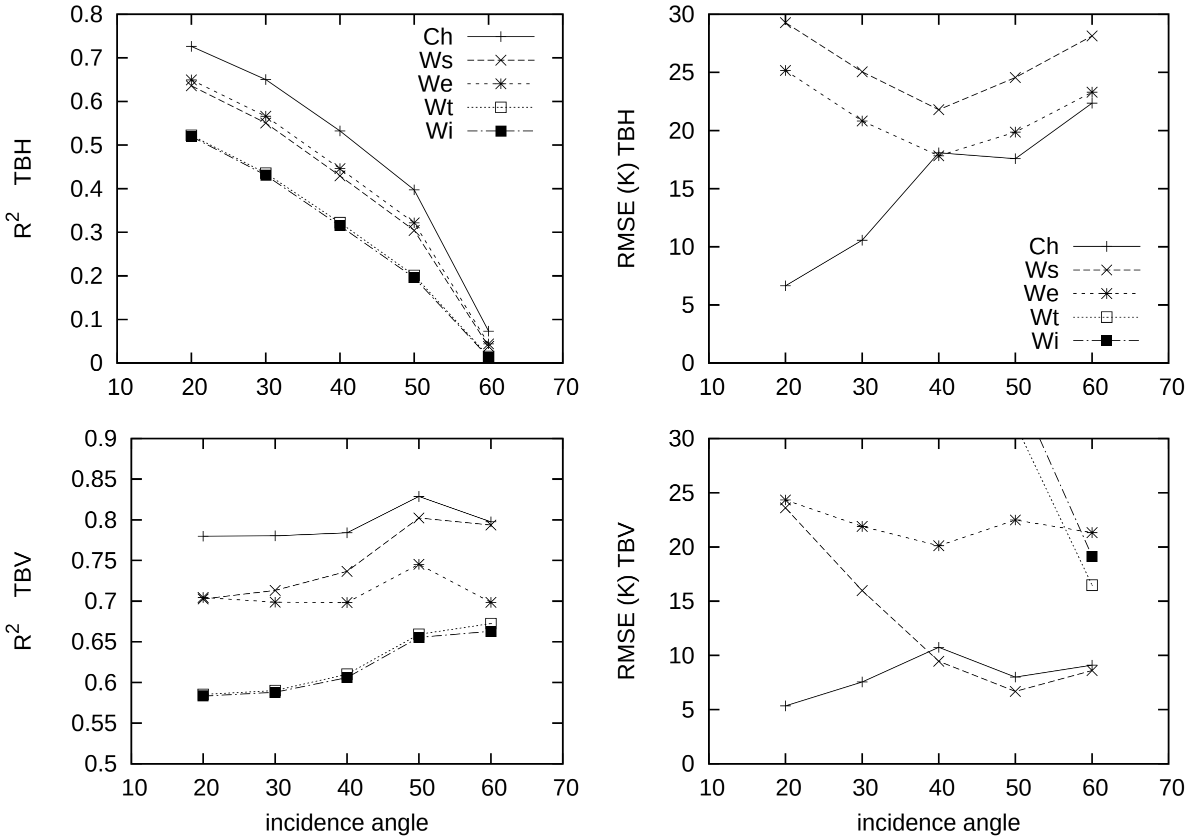

Figure 3: L-band TB background error (R^2 and RMSE) for the year 2004 using different models for soil roughness : Ch= (Choudhury et al., 1979), Ws=(Wigneron et al., 2001), We=(Wegmüller and Mätzler, 1999), Wt=(Laboratories, 2007) and Wi=(Wigneron et al., 2007). The top panels correspond to the H-pol (TBH) and the bottom panels to the V-pol (TBV).

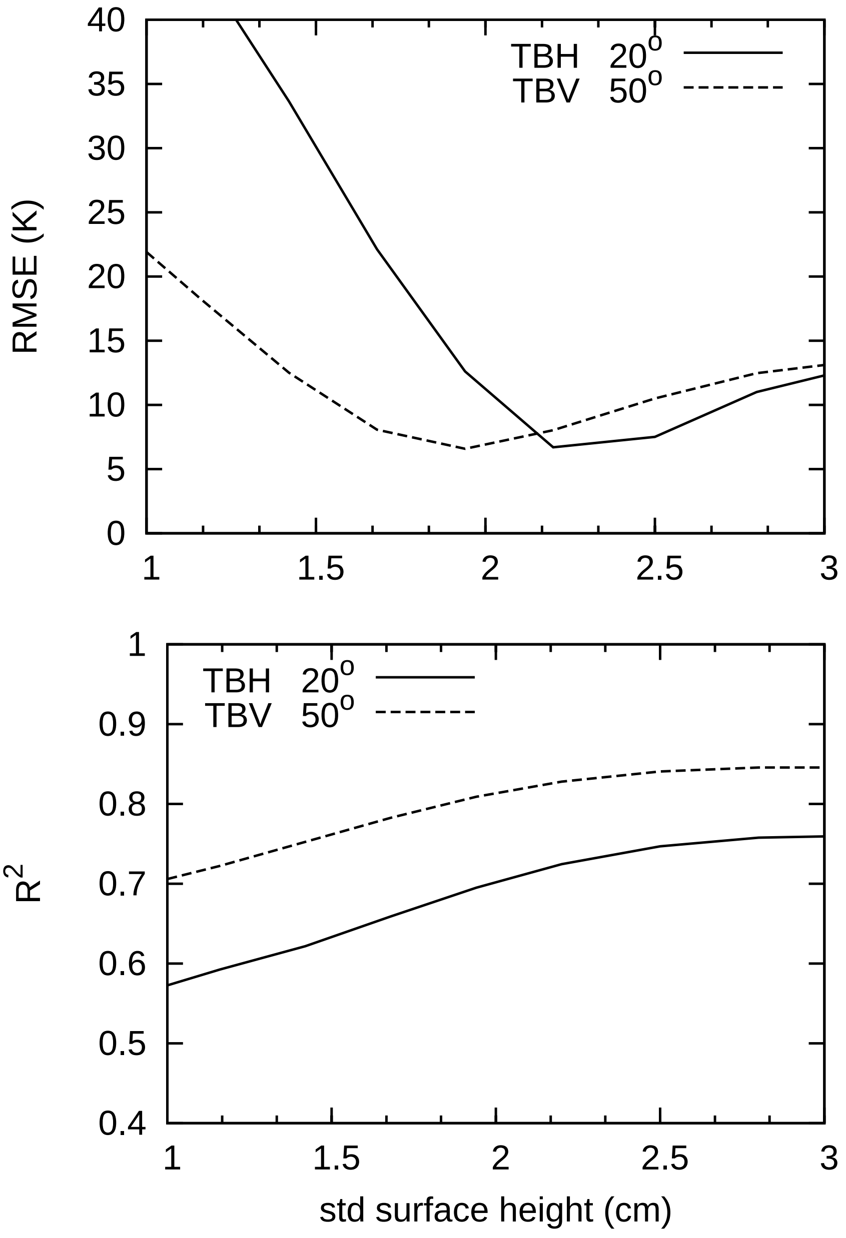

Figure 4: L-band TB background error (RMSE and R^2) as a function of the soil roughness standard deviation height σ. The parameterisation used for soil roughness is Choudhury et al. (1979) for the best incidence angles at each polarisation state.

4 Discussion and conclusions

This study investigates the sensitivity of future operational ECMWF modelled background TB at 1.4 GHz to semi-empirical soil roughness parameterisations available in the ECMWF CMEM forward operator. For this purpose, CMEM is well adapted, and the current available parameterisations for the representation of soil roughness meet NWP requirements.

The analysis carried out in this paper is built on previous studies. One of the main conclusions was that the use of the Kirdyashev et al. (1979) approach to model the effect of the vegetation opacity, in combination with the Wang and Schmugge (1980) model for the soil dielectric contribution, were most suitable to simulate TB in L-band. As a complement to those studies and given the significant contribution of soil roughness to the soil emissivity, this study focuses on soil roughness and investigates which available parameterisation in CMEM is best adapted to simulate TB for NWP applications. The operational forecasted atmospheric fields for the year 2004 are the input forcing for the coupled HTESSEL-CMEM scheme. It is found that for both H-pol and V-pol the Choudhury et al. (1979) simple parameterisation, depending on just the frequency and soil roughness standard deviation of height σ, performs better for most of the tested incidence angles when compared to the available observations. This result confirms that for global scale applications, simple parameterisations are favoured at the expense of more physical based approaches accounting for high resolution land conditions. The performance of first guess TB decreases rapidly with the increase of the incidence angle for H-pol, which is very sensitive to soil water content, whereas less sensitivity is shown at V-pol. Best results are found for V-pol, being also more flexible with regard to the parameterisation used and within the range of all tested incidence angles. Although the parameterisation of Wigneron et al. (2001) for angles greater than 40° at V-pol produced results as good as Choudhury et al. (1979), it is suggested to use Choudhury et al. (1979). Firstly, because it is valid within all the range of tested incidence angles and secondly because this parameterisation is flexible concerning the range of frequency use, widening the possibilities to perform multifrequency NWP data assimilation studies. An important result in this study is that the best incidence angle to minimize background TB errors at L-band is different depending on the polarisation state (20° for H-pol and 50° for V-pol). This makes it possible to discriminate unwanted effects on the microwave signal through the definition of multiangular polarisation rates, as already suggested in Saleh et al. (2006). This is the main driving factor of the multiangular configuration design that will be provided by SMOS observation system.

Background TB at H-pol using the Choudhury et al. (1979) approach for soil roughness are very sensitive to values of the soil roughness parameter h lower than 1.6. For V-pol the soil roughness parameter specification is also important but the dynamical range of variation is lower. Best agreement between modelled and observed TB is found for values of the soil roughness standard deviation of height larger than 2.5 cm. Since the microwave emission is very sensitive to the specification of this empirical parameter, a calibration of this parameter may be performed for SMOS after launch at global scale as a part of a simple bias correction scheme.

The results shown in this paper have some limitations. Due to the scarce availability of validation data sets, in this paper TB simulated with the coupled HTESSEL-CMEM system at 25×25 km horizontal spatial resolution are compared to single point observations obtained at the SMOSREX site. Although the spatial scales under comparison are quite different, a good correlation between the single point observations and the modelled soil moisture and soil temperature fields is shown. The validation site was also shown to be quite representative of the surrounding area. Furthermore, according to the ECOCLIMAP database used in this study, up to a 93% of the vegetation within the grid box analysed in this paper is a C3 grass low vegetation type, the same as at SMOSREX site. Even though single point effects (as mulch effect, water interception by plants or soil moisture influence in the soil roughness) are embedded in the SMOSREX radiometric signal and their effect can be significant, they are likely to be filtered out at coarse resolutions. This might be one source of error when comparing the simulated TB with the observation data set. Another significant source of error (and more relevant for large scale applications) concerns the forecast error, both due to inaccuracies in the forcing meteorological variables such as precipitation or air temperature and to the model physics itself. All this source of errors may affect the local variability of soil moisture. Despite all these limitations, the agreement between modelled TB and the observation system is shown to be reasonably good.

The study carried out in this paper has made it possible to identify a modelling configuration for the soil roughness which reproduces with good accuracy the background TB observed in SMOSREX. The results are very encouraging for using the Choudhury et al. (1979) parameterisation for soil roughness at large scales to obtain global maps of TB. The SMOS satellite will make it possible to validate the CMEM current configuration through first-guess departures monitoring, as well as opening new possibilities to test this and other configurations under very different soil roughness conditions.

Acknowledgements

The authors of this paper would like to thank the SMOSREX team (CESBIO, Météo France, INRA/EPHYSE and ONERA). Many thanks to M. Drusch for the development of CMEM as in the preparation activities for the assimilation of SMOS data in the Integrated Forecast System of the ECMWF.

References

Balsamo, G., P. Viterbo, A. Beljaars, B. van den Hurk, M. Hirschi, A. Betts, and K. Scipal (2009). A revised hydrology for the ECMWF model: Verification from field site to terrestrial water storage and impact in the integrated forecast system. *Journal of Hydrometeorology 10*, 623–643. doi: 10.1175/2008JHM1068.1.

Choudhury, B. J., T. J. Schmugge, A. Chang, and R. W. Newton (1979). Effect of surface roughness on the microwave emission for soils. *Journal of Geophysical Research 84*, 5699–5706.

de Rosnay, P., J. Calvet, Y. Kerr, J. Wigneron, F. Lemaitre, M. Escorihuela, J. M. Sabater, and et al. (2006). SMOSREX: A long term field campaign experiment for soil moisture and land surface processes remote sensing. *Remote Sensing of Environment 102*, 377–389.

de Rosnay, P., M. Drusch, A. Boone, G. Balsamo, B. Decharme, P. Harris, Y. Kerr, T. Pellarin, J. Polcher, and J.-P. Wigneron (2009). AMMA Land Surface Model Intercomparison Experiment coupled to the Community Microwave Emission Model: ALMIP-MEM. *J. Geophys. Res. 114*. D05108, doi:10.1029/2008JD010724.

Drusch, M., T. Holmes, P. de Rosnay, and G. Balsamo (2001). Vegetative and atmospheric corrections for the soil moisture retrieval from passive microwave remote sensing data: Results from the southern great plains hydrology experiment 1997. *J. Hydrometeor. 2*(2), 181–192.

Drusch, M., T. Holmes, P. de Rosnay, and G. Balsamo (2009). Comparing ERA-40 based L-band brightness temperatures with Skylab observations: A calibration / validation study using the Community Microwave Emission Model. *Journal of Hydrometeorology 10*, 213–226. doi: 10.1175/2008JHM964.1.

Drusch, M. and P. Viterbo (2007). Assimilation of screen-level variables in ECMWF's Integrated Forecast System: A study on the impact of the forecast quality and analyzed soil moisture. *Mon. Wea. Rev. 135*(2), 300–314. doi - 10.1175/MWR3309.1.

Eagleman, J. R. and W. C. Lin (1976). Remote sensing of soil moisture by a 21-cm passive radiometer. *Journal of Geophysical Research 81*, 3660–3666.

Engman, E. T. and N. Chauhan (1995). Status of microwave soil moisture measurements with remote sensing. *Remote Sensing of Environment 51*(1), 189–198.

Escorihuela, M., Y. Kerr, P. de Rosnay, J.-P. Wigneron, J.-C.Calvet, and F. Lemaitre (2007). A simple model of the bare soil microwave emission at l-band. *IEEE Transactions on Geoscience and Remote Sensing 45*(7), 1978–1987.

Fischer, E., S. Seneviratne, P. Vidale, D. Luthi, and C. Schr (2007). Soil moisture-atmosphere interactions during the 2003 european summer heat wave. *Journal of Climate 20*(20), 5081–5099. doi: 10.1175/JCLI4288.1.

Gruhier, C., P. de Rosnay, Y. Kerr, E. Mougin, E. Ceschia, J.-C.Calvet, and P. Richaume (2008). Evaluation of AMSR-E soil moisture product based on ground measurements over temperate and semi-arid regions. *Geophysical Research Letters*. doi: 10.1029/2008GL033330.

Holmes, T., M. Drusch, J.-P. Wigneron, and R. de Jeu (2008). A global simulation of microwave emission: Error structures based on output from ECMWFS operational integrated forecast system. *IEEE Transactions on Geoscience and Remote Sensing 46*(3, doi:10.1109/TGRS.2007.914798), 846 – 856.

Jones, A., T. Vukicevic, and T. V. Haar (2004). A microwave satellite observational operator for variational data assimilation of soil moisture. *Journal of Hydrometeorology 5*, 213–229.

Kerr, Y., P. Waldteufel, J.-P. Wigneron, J.-M. Martinuzzi, J. Font, and M. Berger (2001). Soil moisture retrieval from space: The soil moisture and ocean salinity (SMOS) mission. *IEEE Trans. Geosc. Remote Sens. 39*(8), 1729–1735.

Kirdyashev, K., A. Chukhlantsev, and A. Shutko (1979). Microwave radiation of the earth's surface in the presence of vegetation cover. *Radiotekhnika i Elektronika 24*, 256–264.

Laboratories, S. E. S. (2007). SMOS level-2 processor for soil moisture algorithm theoretical based document (ATBD). Technical report, SO-TN-ESL-SM-GS-0001. issue 2.a, p.124.

Lemaitre, F., J. Poussire, Y. Kerr, M. Dejus, R. Durbe, and P. de Rosnay et al. (2004). Design and test of the ground based L-band radiometer for estimating water in soils (LEWIS). *IEEE Trans. Geosc. Remote Sens. 42*(8), 1666–1676.

Masson, V., J.-L. Champeaux, F. Chauvin, C. Meriguet, and R. Lacaze (2003). A global database of land surface parameters at 1-km resolution in meteorological and climate models. *Journal of Climate 16*, 1261–1282.

Njoku, E. and D. Entekhabi (1996). Passive microwave remote sensing of soil moisture. *Journal of Hydrometeorology 184*(1-2), 101–129.

Pellarin, T., J.-P. Wigneron, J.-C. Calvet, and P. Waldteufel (2003). Global soil moisture retrieval from a synthetic l-band brightness temperature data set. *Journal of Geophysical Research 108*(4364, doi:10.1029/2002JD003086).

Sabater, J. M., C.Rüdiger, J. Calvet, N. Fritz, L.Jarlan, and Y.Kerr (2008). Joint assimilation of surface soil moisture and lai observations into a land surface model. *Agricultural and Forest Meteorology 148*, 1362–1373.

Sabater, J. M., L. Jarlan, J. Calvet, F. Bouyssel, and P. de Rosnay (2007). From near surface to root-zone soil moisture using different assimilation techniques. *Journal of Hydrometeorology 8*(2), 194–206.

Saleh, K., J.-P. Wigneron, P. de Rosnay, J.-C. Calvet, and Y. Kerr (2006). Semi-empirical regressions at L-band applied to surface soil moisture retrievals over grass. *Remote Sensing of Environment 101*(3), 415–426.

Salgado, R. (1999). Global soil maps of sand and clay fractions and of the soil depth for MESONH simulation based on FAO/UNESCO soil maps. Technical report, CNRM/Météo France. Tech. Note, **59**.

Schneeberger, K., M. Schwank, C. Stamm, P. de Rosnay, C. Mätzler, and H. Flühler (2004). Topsoil structure influencing soil water retrieval by microwave radiometry. *Vadose Zone Journal 3*, 1169–1179.

Shi, J., K. Chen, Q. Li, T. Jackson, P. Neill, and L. Tsang (2002). A parameterized surface reflectivity model and estimation of bare-surface soil moisture with L-band radiometer. *IEEE Trans. Geosc. Remote Sens. 40*(12), 2674–2686.

Wang, J. R. and B. J. Choudhury (1981). Remote sensing of soil moisture content over bare field at 1.4 ghz frequency. *Journal of Geophysical Research 86*, 5277–5282.

Wang, J. R. and T. Schmugge (1980). An empirical model for the complex dielectric permittivity of soils as a function of water content. *IEEE Transactions on Geoscience and Remote Sensing 18*, 288–295.

Wegmüller, U. and C. Mätzler (1999). Rough bare soil reflectivity model. *IEEE Transactions on Geoscience and Remote Sensing 37*, 1391–1395.

Wigneron, J.-P., Y. Kerr, P. Waldteufel, K. Saleh, M.-J. Escorihuela, P. Richaume, P. Ferrazzoli, P. de Rosnay, R. Gurneye, J.-C. Calvet, J. Grant, M. Guglielmetti, B. Hornbuckle, C. Mtzler, T. Pellarin, and M. Schwank (2007). L-band microwave emission of the biosphere (L-MEB) model: Description and calibration against experimental data sets over crop fields. *Remote Sensing of Environment 107*(4), 639–655.

Wigneron, J. P., L. Laguerre, and Y. Kerr (2001). A simple parameterization of the L-band microwave emission from rough agricultural soils. *IEEE Transactions on Geoscience and Remote Sensing 39*, 1697–1707.